SHORT COMMUNICATION

Inhibition of lysosomal Ca²⁺ signalling disrupts dendritic spine structure and impairs wound healing in neurons

Zahid Padamsey [†], Lindsay McGuinness[†], and Nigel J. Emptage

Department of Pharmacology, University of Oxford, Oxford, UK

ABSTRACT

A growing body of evidence suggests that lysosomes, which have traditionally been regarded as degradative organelles, can function as Ca²⁺ stores, regulated by the second messenger nicotinic acid adenine dinucleotide phosphate (NAADP). We previously demonstrated that in hippocampal pyramidal neurons, activity-dependent Ca²⁺ release from these stores triggers fusion of the lysosome with the plasma membrane. We found that the physiological role of this Ca²⁺-dependent fusion was to maintain the long-term structural enlargement of dendritic spines induced by synaptic activity. Here, we examined the pathophysiological consequences of lysosomal dysfunction in hippocampal pyramidal neurons by chronically inhibiting lysosomal Ca²⁺ signalling using the NAADP antagonist, NED-19. We found that within just 20 hours, inhibition of lysosomal function led to a profound intracellular accumulation of lysosomal membrane. This was accompanied by a significant change in dendritic spine structure, which included a lengthening of dendritic spines, an increase in the number of filipodia, and an overall decrease in spine number. Inhibition of lysosomal function also inhibited wound healing in neurons by preventing lysosomal fusion with the plasma membrane. Neurons were therefore more susceptible to injury. Our findings suggest that dysfunction in lysosomal Ca²⁺ signalling and lysosomal fusion with the plasma membrane may contribute to the loss of dendritic spines and neurons seen in neurological disorders, such as Niemann-Pick disease type C1, in which lysosomal function is impaired.

NAADP is a second messenger necessary for the mobilization of Ca²⁺ from lysosomes and lysosome-related related organelles (collectively referred to here as lysosomes).[1,2] We have previously demonstrated that back-propagating action potentials trigger a NAADP-dependent release of Ca²⁺ from lysosomes in hippocampal dendrites, which in turn, triggers fusion of the lysosome with the plasma membrane.[3] This fusion results in the release of the lysosomal protease Cathepsin B, which, via activation of matrix metalloproteinase 9 (MMP-9), is essential for maintaining activity-dependent enlargements of dendritic spines induced by synaptic activity. We found that acute application of NED-19, a NAADP antagonist that blocks Ca²⁺ release from the lysosomes, inhibited the fusion of the lysosome to the plasma membrane and prevented the long-term maintenance of activity-dependent spine growth.

Given that lysosomal dysfunction is implicated in a number of neurological diseases,[4] we sought to examine the effects of chronic inhibition of lysosomal Ca²⁺ signalling with NED-19 on neuronal and synaptic function. We first confirmed that prolonged treatment (16–20 hours) of hippocampal slices with NED-19 (100 μM) resulted in a chronic impairment of activity-dependent lysosomal Ca²⁺ signalling in neuronal dendrites (Fig. 1A). We found that in slices incubated with a single dose of NED-19 (100 μM) for 20 hours, action potential evoked Ca²⁺ influx was significantly reduced compared to controls (Fig. 1B; p < 0.01). Subsequent addition of GPN (Fig. 1B), which disrupts lysosomal Ca²⁺ storage by perforation of the lysosome membrane,[1] resulted in no further reduction of Ca²⁺ signalling, suggesting that NED-19 treatment abolished activity-dependent lysosomal Ca²⁺ signalling.
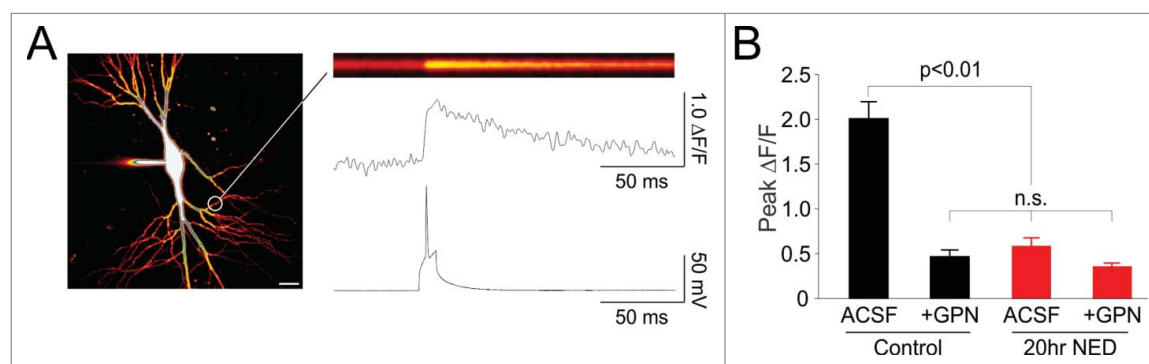
Since inhibition of lysosomal Ca²⁺ signalling in hippocampal neurons impairs fusion of the lysosome with the plasma membrane,[3] we next examined whether prolonged treatment with NED-19 had any obvious effect on the intracellular distribution of lysosomes. We incubated primary hippocampal cultures with NED-19 (10 μm, dissolved in DMSO) for 16–20 hours, after which we labelled lysosomes fluorescently using LysoTracker Green.

Figure 1. Chronic incubation with NED-19 impairs activity-dependent lysosomal Ca^{2+} signalling in hippocampal neurons. (A) Left. CA1 hippocampal pyramidal neuron recorded with whole-cell patch clamp and loaded with the Ca^{2+} sensitive dye Oregon Green BAPTA-1 (scale bar = 5 μm). Confocal laser scanning was restricted to a line across a region of dendrite (white circle). (B) Example line scan image showing dendritic Ca^{2+} influx in response to an action potential, generated by somatic current injection. The line scan is quantified ($\Delta F/F$) below, and time-locked to the simultaneously recorded membrane potential. (B) Peak action potential-evoked Ca^{2+} transient recorded in the dendrites across conditions (ACSF = artificial cerebrospinal fluid). GPN, which disrupts lysosomal membranes, reduced Ca^{2+} signalling under control conditions, but not following a 20 hour treatment with NED-19, suggesting that chronic NED-19 incubation successfully abolished activity-dependent lysosomal Ca^{2+} signalling. Error bars represent S.E.M. (n = 8–13 dendrites/condition). Non-significant group comparisons are denoted by n.s.

We found that NED-19 greatly enhanced the amount of lysosomes present in neurons compared to vehicle control (DMSO) (Fig. 2A, Bii; p < 0.01). Under electron microscopy (EM), lysosome enlargement was clearly evident in NED-19 treated cells, and manifested as large multi-lamellar vesicular bodies (Fig. 2C, D; p < 0.05). Similar increases in lysosomal number and size have been reported in some lysosome storage disorders.[5]

We reasoned that the accumulation of lysosomal membrane may have resulted from impairments of lysosomal fusion with the plasma membrane induced by NED-19[3]. However, accumulation may have alternatively arisen from an impairment in lysosomal fusion in the endocytosis pathway. To examine this possibility, we briefly (10–15 minutes) exposed cell cultures to FM 4–64 to fluorescently label early recycling endosomes (Fig. 2A). We then examined fluorescence 16 hours later. In both control and NED-19 treated cultures, the FM-dye ended up in the lysosomes, as quantified by co-localization between FM-dye and Lysotracker staining (Fig. 2A, Bi). Thus, recycling endosomes were eventually able to fuse with, or mature into, lysosomes, suggesting that endocytic pathway function was likely preserved in NED-19. However, it is important to note that our assay has limited sensitivity and would only be expected to detect gross defects in intracellular trafficking. We may therefore be unable to detect the less pronounced deficits that are associated with some lysosomal storage disorders.[6,7] Nonetheless, our findings suggest that NED-19 induced accumulation of lysosomal membrane likely did not result from a deficit for endosomes to fuse with lysosomes. Although this suggests that lysosomal accumulation may have resulted from impairments in lysosomal fusion with the plasma membrane, we cannot rule out that potential, NED-19 induced deficits in lysosomal autophagy may also play a role. Indeed, many lysosomal storage disorders are associated with a deficiency in lysosomal hydrolase activity, which impairs autophagy and the break-down of macromolecules, leading to an accumulation of lysosomal membrane and undigested substrates.[7,8]

In our previous work, we demonstrated that lysosomal fusion to the plasma membrane was essential for maintaining activity-dependent spine growth.[3] A chronic impairment of fusion may therefore alter spine structure. To investigate, we examined dendritic spines of CA3 and CA1 pyramidal neurons in hippocampal slice cultures chronically treated with NED-19 (Fig. 3A). Within 16–20 hours, NED-19 produced significant changes in spine structure and number that was not observed with more acute applications (<2 hours[3]). These changes included an increase in spine length (Fig. 3B; p < 0.01), an outgrowth of filipodia (Fig. 3C; p < 0.05), and a reduction in spine density (Fig. 3D; p < 0.05). These characteristics are reminiscent of structural changes induced by long-term depression (LTD).[9] Given our previous findings that lysosomal fusion is necessary for the maintenance of spine enlargements associated with LTP induction, the phenotype induced by NED-19 may emerge owing to a dominance of LTD over LTP.

We also examined the effect of chronic lysosome dysfunction on cell health. We found no obvious change in cell health as assessed by cell electrophysiology and morphology in slice cultures treated for 16–20 hours with NED-19 (data not shown). We therefore turned to examining the susceptibility of neurons to stress. It is known that Ca^{2+}-dependent exocytosis of lysosomes in
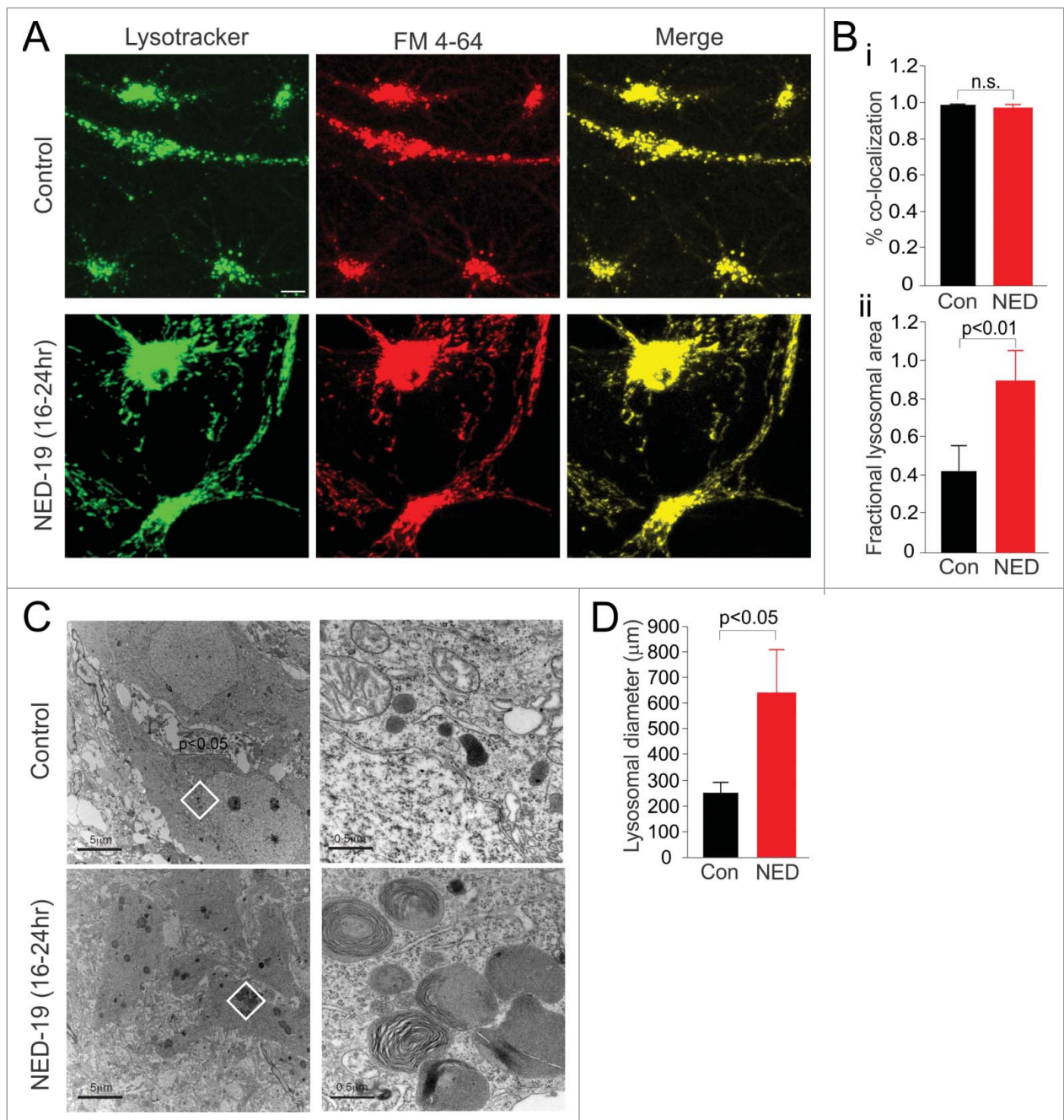
Figure 2. Chronic incubation with NED-19 results in an accumulation of lysosomal membrane, but does not impair the endocytic pathway. (A) NED-19 treatment resulted in an increase in the amount of Lysotracker-labelled lysosomes (green) compared to vehicle control (Con). In both control and NED-19 treated cells, FM 4–64 (red) loading in recycling endosomes co-localized (yellow) with Lysotracker after 16–20 hours, suggesting normal function in the endocytic pathway (scale bar = 5 μm). (Bi) Quantification of co-localization of FM 4–64 and Lysotracker staining. (Bii) Quantification of lysosomal area. (C). EM images. Multi-lamellar vesicular bodies were observed in the cell cytosol of NED-19 treated cells. (D) Quantification of lysosome diameter from EM images. (Left) Scale bar = 5 μm. Image in the white region is magnified 10x on the right. (Right) Scale bar = 0.5 μm. Error bars represent S.E.M. (n = 6–10 cells/condition). Non-significant group comparisons are denoted by n.s.

fibroblasts plays an important role in resealing their plasma membrane after injury.[10-12] We considered that lysosomes may have a similar role in neurons, and reasoned that if it were the case, inhibiting lysosomal fusion using NED-19 should impair wound healing. To test this, we wounded neurons by using by using a pressurized biolistic gene gun to shoot gold particles at hippocampal slice cultures. This was done in the presence of extracellularly applied fluorescein-dextran, which being membrane impermeable, would only enter and remain in wounded cells that successfully were able to reseal their membranes.[13] Consequently, fluorescent
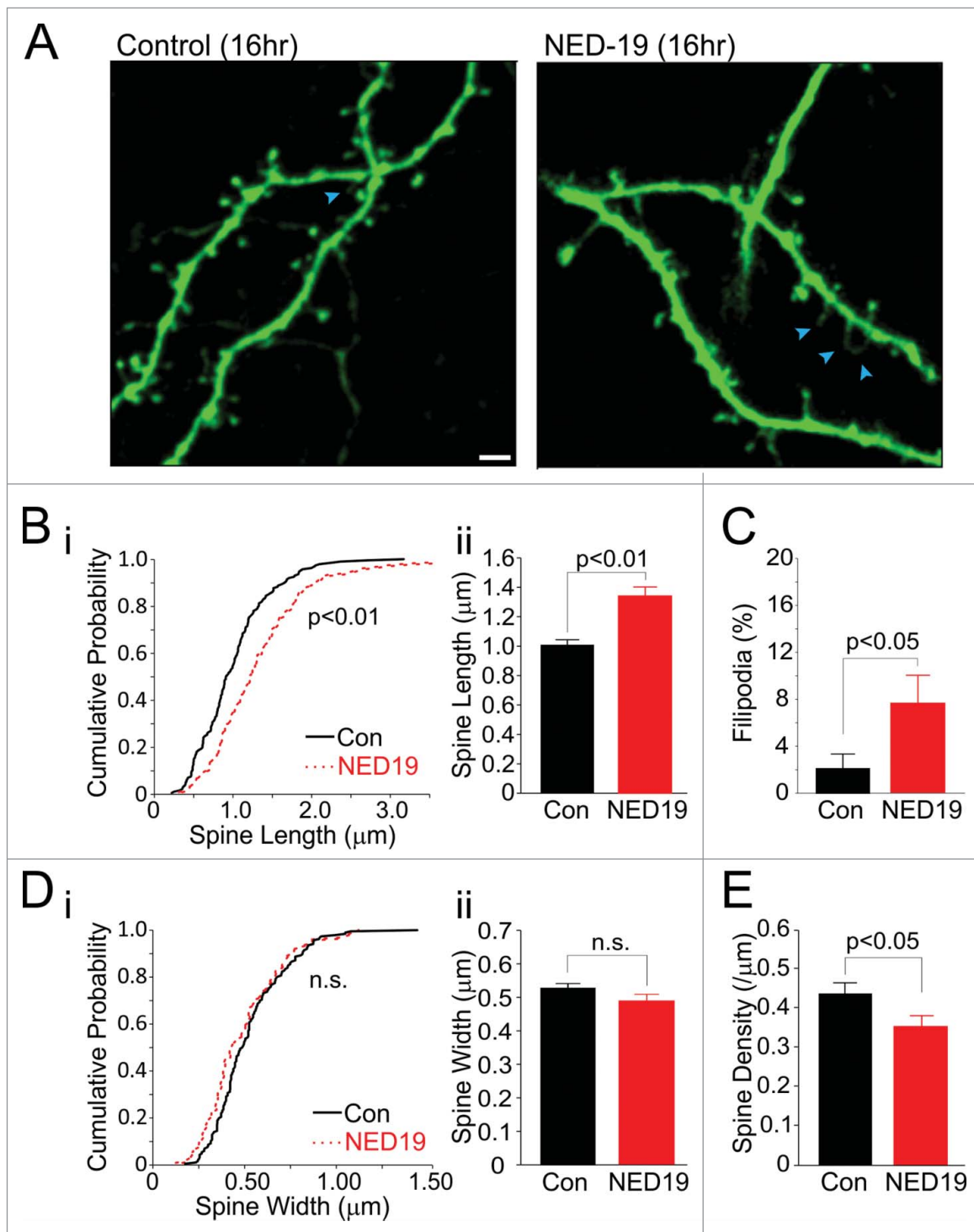
Figure 3. Chronic incubation with NED-19 alters spine morphology. (A) Sample images of pyramidal dendrites under control conditions (Con) or following a 16–20 hour incubation with NED-19 (scale bar = 2 μm). As compared with vehicle controls, NED-19-treated cells have a larger portion of filipodia (blue arrows) and a larger number of spines with long necks. (B) (i) Cumulative probability plot and (ii) averages of spine lengths (n = 144–186 spines/condition). Neck length was significantly increased with NED-19 treatment. (C) Percentage filipodia was significantly increased with NED-19 treatment (n = 144–186 spines/ condition). (D) (i) Cumulative probability plot and (ii) averages of spine widths (n = 144–186 spines/condition). Spine width was unchanged with NED-19 treatment. (E) Spine density was decreased with NED-19 treatment (n = 23–24 dendrites/condition). Error bars represent S.E.M. Non-significant group comparisons are denoted by n.s.

labelling would be positively correlated with wound healing. Using this technique, we found that even an acute application of NED-19 (<2 hours) significantly decreased the proportion of labelled pyramidal cells compared to vehicle controls (DMSO) (Fig. 4A, B; p < 0.01). We repeated our experiments using GPN (100 μM, dissolved in DMSO) and monensin (20 μM, dissolved in ethanol) to disrupt lysosomal Ca^{2+} signalling, which work via mechanisms different to NED-19. GPN results in the perforation of lysosomal membrane (Fig. 4B).[1] Monensin is a membrane-permeable Na^+/H^+ ionophore that disrupts the lysosomal proton gradient

necessary for sequestering Ca^{2+} within the organelle.[1] Despite different mechanisms of actions, both drugs produced similar effects to NED-19, suggesting that they too impaired wound healing (Fig. 4A, B; p < 0.01).

To confirm that wound healing was recruiting lysosomal membrane, we used LAMP2-pHlourin to directly image lysosomal fusion in real-time during mechanical injury.[3] LAMP2-pHlourin consists of a pH-sensitive variant of green fluorescent protein (GFP) that has been fused to the luminal domain the lysosome-associated membrane protein, LAMP-2. The fluorescence of the GFP is quenched in the acidic domain of the lysosome,
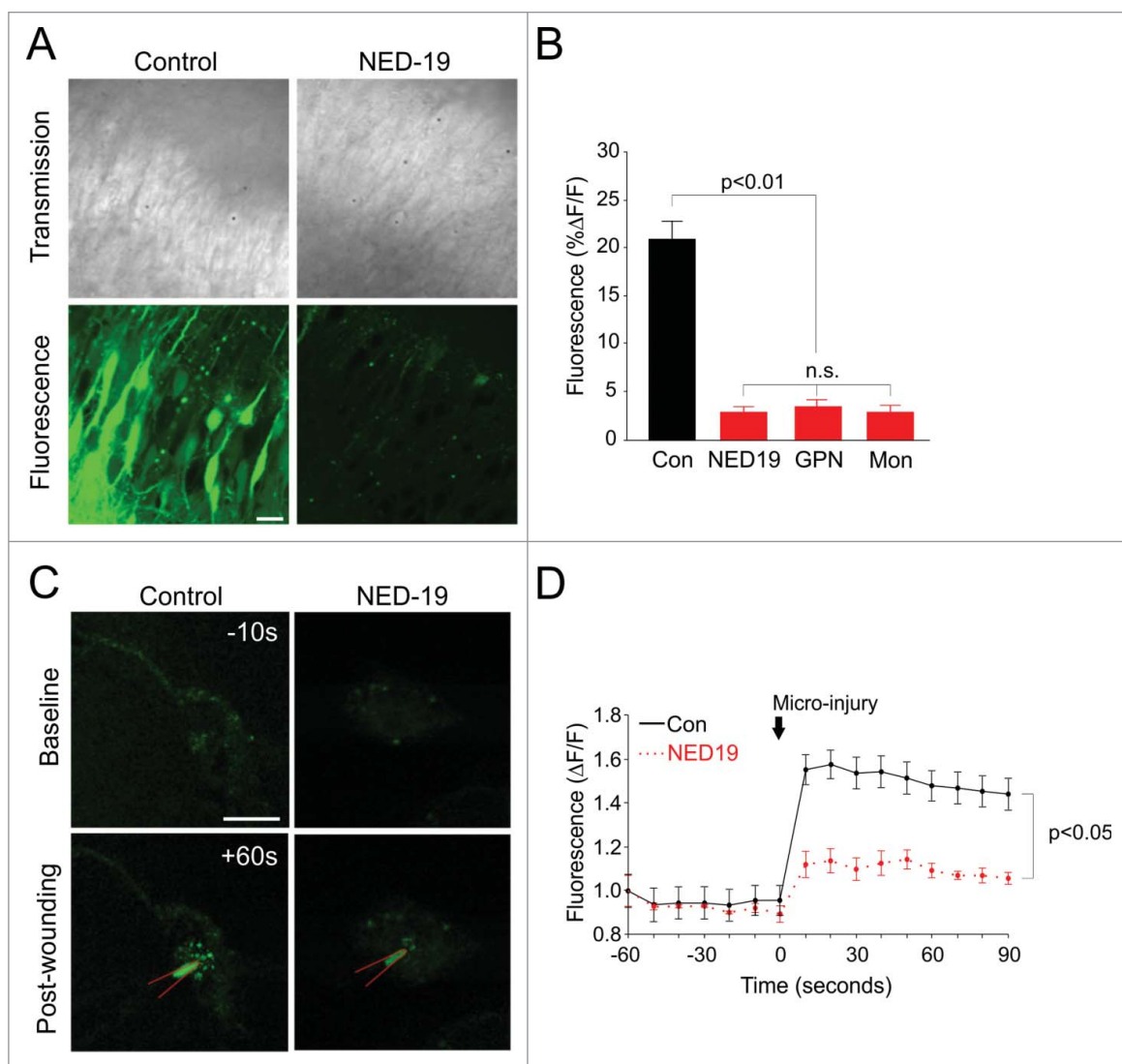
Figure 4. NED-19 compromises plasma membrane repair by preventing lysosomal fusion with the plasma membrane. (A) Sample transmission (top) and fluorescent (bottom) images of pyramidal cells in hippocampal slice cultures incubated with fluoroscein dextran during biolistic wounding. Only cells that have successfully re-sealed cells become fluorescently labelled. Pre-treatment with Ned-19, GPN, or Mon (monensin) abolished fluorescent labelling seen in vehicle control (Con), suggesting that membrane repair was compromised. Scale bar = 10 μm. (B) Quantification of fluoroscein dextran fluorescent labelling (n > 5 slices/condition). (C) Sample image of dissociated neurons transfected with LAMP2-pHlourin prior to and following wounding with a sharp microelectrode (red). Local fluorescence increase was triggered by wounding in control conditions, and reduced with NED-19 treatment. Scale bar = 10 μm (D). Quantification of LAMP2-pHlourin fluorescence over time (n = 3 cells/condition). Error bars represent S.E.M. Non-significant group comparisons are denoted by n.s.

but is unmasked when exposed to the relatively pH neutral environment of the extracellular fluid, which occurs when the lysosome fuses with the plasma membrane. Hippocampal primary cultures were transfected with LAMP2-pHlourin and targeted for micro-injury using a sharp glass micropipette (80-120 MΩ). Following wounding, we observed a rapid and local increase of fluorescence in the vicinity of the sharp micro-electrode, suggesting that lysosomes were fusing with the plasma membrane at the site of injury (Fig. 4C, D; $p < 0.05$). Pre-treating cells with NED-19 significantly reduced this fluorescent increase, though did not quite abolish it (Fig. 4C, D; $p < 0.05$). This suggests that although lysosomal Ca^{2+} signalling contributes to wound healing, other sources of Ca^{2+}, such as Ca^{2+} influx from the extracellular fluid, are also likely to play a role. To our knowledge, we are the first to demonstrate that the lysosomes mediate the wound healing response in neurons, as in fibroblasts,[10-12] and that Ca^{2+} release from the lysosome itself is important for the process.

Dysfunction in lysosomal Ca^{2+} signalling is thought to play a role in lipid storage disorders.[14-16] In the case of Niemann-Pick disease type C1 (NPC), it has been shown that dysfunction of the NPC1 protein causes a reduction in lysosomal Ca^{2+} storage and release owing to accumulation of sphingosine in the lysosome. Lysosomal Ca^{2+} dysfunction, in turn, leads to hallmark NPC cellular phenotypes, including the secondary storage of sphingolipids and cholesterol.[14] NPC is also associated with neuronal dysfunction.[17] In our study, we found that disrupting lysosomal Ca^{2+} signalling with NED-19 resulted in a lengthening of spines, an outgrowth of filipodia, and a reduction in synaptic density. Incidentally, comparable synaptic changes have been reported in animal models of NPC and related lipid storage disorders.[18-20] We also found that NED-19 treated cells had an impaired ability to repair damaged membranes, which may also contribute to the accelerated cell loss seen in these diseases.[21] Thus, inhibition of lysosomal signalling may underlie some of the neurological phenotypes reported in NPC and related disorders. Lysosomal dysfunction has also been reported in a number of other neurological diseases, such as Alzheimer's, Parkinson's, and Huntington's,[4] and our findings may also apply to these disorders; however, whether lysosomal Ca^{2+} signalling and lysosomal fusion with the plasma membrane are impaired in these diseases remains to be elucidated.[4]

Methods

Cell cultures

All animal work was carried out in accordance with the Animals (Scientific Procedures) Act, 1986 (UK) and under project and personal licenses approved by the Home Office (UK). Cultured hippocampal slices (350 μm) and dissociated cultures, hippocampal cells were prepared and used as described in (Padamsey et al., 2017).[3] All experiments were conducted DIV 14–21 in Tyrodes solution (in mM: 128 NaCl, 5 KCl, 1 $MgCl_2$, 2 $CaCl_2$, 4.2 $NaHCO_3$, 20 glucose and 15 HEPES; pH = 7.2–7.4; 22–24°C).

Ca^{2+} imaging

Ca^{2+} imaging was conducted as in (Padamsey et al., 2017).[3] Briefly, CA1 pyramidal neurons were recorded using patch electrodes (4-8M) filled with internal solution (in mM: 135 KGluconate, 10 KCl, 10 HEPES, 2 $MgCl_2$, 2 Na_2ATP and 0.4 Na_3GTP) containing 200 μM Oregon Green BAPTA-1 (ThermoFisher). Electrophysiological data was acquired with an Axoclamp 2A amplifier (Axon Insturments), recorded with WinWCP (Strathclyde Electrophysiology Software) and analysed with Clampfit (Axon Insturments) and Excel (Microsoft). Data was acquired at 3 kHz and sampled at 10 kHz. Confocal images were acquired using a BioRad MRC-1000 confocal laser scanning system, equipped with a 488 nm argon line, and LaserSharp software. Images were acquired through a 60x water-immersion objective (Olympus; 0.9 NA). Line scans were taken though apical dendrites at 500 Hz. Action potentials were evoked using a 10 ms current injection of 1.0-2.0 nA. Fluorescent changes were quantified as $\Delta F/F = (F - F_{baseline}/ F_{baseline - background})$ using ImageJ and Excel.

Lysosome labelling

LysoTracker was used as per manufacturer's instructions to label lysosomes. Briefly, cells were incubated with 50–75 nM LysoTracker Green (dissolved in DMSO) for 1–2 hours. Recycling endosomes were labelled by applying FM 4–64 (10 uM; dissolved in distilled water) for 10–15 minutes. LAMP2-pHlourin was made, transfected, and imaged as described in (Padamsey et al., 2017).[3]

Dendritic spine imaging

Dendritic spines were imaged in slice cultures biolistically transfected with enhanced green fluorescence protein (eGFP, Clontech) using the Helios Gene Gun System (Bio-Rad), as per manufacturer's instructions. 1.6 μm diameter gold microcarriers were loaded with DNA in a ratio of ∼1.7 μg DNA/mg gold and shot at 120 psi. Gold without DNA was shot at 220 psi for biolistic wounding. In wounding experiments, slices were incubated with fluoroscein dextran (10 000 MW, 5 mg/

mL in PBS; Sigma) for 30 minutes prior to biolistic wounding, and then subsequently rinsed for 10 minutes before imaging. All images were acquired on a confocal microscope (BioRad MRC-1000) through a 60x water-immersion objective (Olympus; 0.9 NA) and using z-stacks (0.5 μm step-size, 512 $\times$ 512 resolution). Images were analysed using ImageJ and Excel.

Electron microscopy

Hippocampal slice cultures were maintained in culture for 7 days prior to preparation for EM. Ned-19 treated slices were incubated with drug for 16–20 hours before fixation. The slices, attached to their membrane insert, were immersion fixed (3% glutaraldehyde in 0.1M sodium phosphate buffer) on ice for 3 hours, transferred into 2M sucrose solution in 0.1M phosphate buffer (PB) (pH7.2) then post fixed in 1% osmium tetroxide (0.1M PB, 2M sucrose) for 2 hours at room temperature. Rinsed briefly in 0.1M PB sucrose buffer and several changes of 50% then 70% ethanol to remove phosphate ions, they were incubated in 1% uranyl acetate in 70% ethanol for 30 minutes in the dark at room temperature. The inserts were removed from frames and hippocampal slices were transferred to glass vials for the remainder of processing. The slices were subsequently dehydrated through a graded series of ethanol followed by propylene oxide, propylene oxide: resin (50:50) and then 100% TAAB embedding resin. (TAAB Laboratories Equipment Ltd) prior to embedding in fresh TAAB resin on a tilting platform to assist with penetration of resin overnight. The resin was exchanged and slices infiltrated for a further 2 hours, before mounting onto slides. They were allowed to flatten for 2 hours under coverslips on a hot plate before polymerisation for 48 hrs at 60°C. After photography at the light microscopy level, regions of interest were cut from the flat embedded tissue and mounted on the tips of resin blocks. Ultrathin sections of these regions (∼70 nm) were cut with a diamond knife (Diatome; TAAB; UK) on a Reichert-Jung Ultracut E and collected on pioloform coated copper single slot grids. The sections on grids were counterstained with lead citrate (Reynolds, 1963) before examination using a Philips CM10 electron microscope attached to a Gatan Bioscan Digital camera (Gatan, UK).

Statistics

Statistical significance was assessed using two-tailed Mann-Whitney tests when data was not normally distributed as assessed by a test for sphericity, otherwise two-tailed, unpaired t-tests were used. One sample z-tests were used to assess significant differences from a given value. Kolmogorov-Smirnov test was used to test significance between cumulative distributions. ANOVA and post-hoc Bonferroni tests were used to assess the significance of multiple comparisons for normally distributed data. p-values of significant comparisons are clearly stated on the figures.

Disclosure of potential conflicts of interest

No potential conflicts of interest were disclosed.

Funding

ORCID

Zahid Padamsey   http://orcid.org/0000-0001-9177-8210
Nigel J. Emptage   http://orcid.org/0000-0002-7348-497X

References

[1] Morgan AJ, Davis LC, Galione A. Imaging approaches to measuring lysosomal calcium. Methods Cell Biol. 2015;126:159-195. doi:10.1016/bs.mcb.2014.10.031.

[2] Galione A. A primer of NAADP-mediated Ca signalling: From sea urchin eggs to mammalian cells. Cell Calcium. 2014. doi: S0143-4160(14)00155-9 [pii] 10.1016/j.ceca.2014.09.010. PMID:25449298

[3] Padamsey Z, McGuinness L, Bardo SJ, Reinhart M, Tong R, Hedegaard A, Hart ML, Emptage NJ, et al. Activity-dependent exocytosis of lysosomes regulates the structural plasticity of dendritic spines. Neuron. 2017;93:132-146, doi:10.1016/j.neuron.2016.11.013.

[4] Zhang L, Sheng R, Qin Z. The lysosome and neurodegenerative diseases. Acta Biochim Biophys Sin (Shanghai). 2009;41:437-445. doi:10.1093/abbs/gmp031. PMID: 19499146

[5] Otomo T, Higaki K, Nanba E, Ozono K, Sakai N. Lysosomal storage causes cellular dysfunction in mucolipidosis II skin fibroblasts. J Biol Chem. 2011;286:35283-35290. doi:10.1074/jbc.M111.267930. PMID:21846724

[6] Pryor PR, Reimann F, Gribble FM, Luzio JP. Mucolipin-1 is a lysosomal membrane protein required for intracellular lactosylceramide traffic. Traffic. 2006;7:1388-1398. doi:10.1111/j.1600-0854.2006.00475.x. PMID:16978393

[7] Futerman AH, van Meer G. The cell biology of lysosomal storage disorders. Nat Rev Mol Cell Biol. 2004;5:554-565. http://www.nature.com/nrm/journal/v5/n7/suppinfo/nrm1423_S1.html. doi:10.1038/nrm1423. PMID:15232573

[8] Settembre C, Fraldi A, Jahreiss L, Spampanato C, Venturi C, Medina D, de Pablo R, Tacchetti C, Rubinsztein DC, Ballabio A. A block of autophagy in lysosomal storage disorders. Hum Mol Genet. 2008;17:119-129. doi:10.1093/hmg/ddm289. PMID:17913701

[9] Segal M. Dendritic spines and long-term plasticity. Nat Rev Neurosci. 2005;6:277-284. doi:10.1038/nrn1649. PMID:15803159

[10] Rodriguez A, Martinez I, Chung A, Berlot CH, Andrews NW. cAMP regulates Ca2+-dependent exocytosis of lysosomes and lysosome-mediated cell invasion by trypanosomes. J Biol Chem. 1999;274:16754-16759. doi:10.1074/jbc.274.24.16754. PMID:10358016

[11] Rodriguez A, Webster P, Ortego J, Andrews NW. Lysosomes behave as Ca2+-regulated exocytic vesicles in fibroblasts and epithelial cells. J Cell Biol. 1997;137:93-104. doi:10.1083/jcb.137.1.93. PMID:9105039

[12] Reddy A, Caler EV, Andrews NW. Plasma membrane repair is mediated by Ca(2+)-regulated exocytosis of lysosomes. Cell. 2001;106:157-169. doi:10.1016/S0092-8674(01)00421-4. PMID:11511344

[13] McNeil PL. Direct introduction of molecules into cells. Current protocols in cell biology 2001;20.1:1-7. doi:10.1002/0471143030.cb2001s18. PMID:18228351

[14] Lloyd-Evans E, Morgan AJ, He X, Smith DA, Elliot-Smith E, Sillence DJ, Churchill GC, Schuchman EH, Galione A, Platt FM. Niemann-Pick disease type C1 is a sphingosine storage disease that causes deregulation of lysosomal calcium. Nat Med. 2008;14:1247-1255. doi:10.1038/nm.1876. PMID:18953351

[15] Lloyd-Evans E, Platt FM. Lysosomal Ca(2+) homeostasis: role in pathogenesis of lysosomal storage diseases.

Cell Calcium. 2011;50:200-205. doi:10.1016/j.ceca.2011.03.010. PMID:21724254

[16] Morgan AJ, Platt FM, Lloyd-Evans E, Galione A. Molecular mechanisms of endolysosomal Ca2+ signalling in health and disease. Biochem J. 2011;439:349-374, doi:BJ20110949 [pii] 10.1042/BJ20110949.doi:10.1042/BJ20110949. PMID:21992097

[17] Lloyd-Evans E, Platt FM. Lipids on trial: the search for the offending metabolite in Niemann-Pick type C disease. Traffic. 2010;11:419-428. doi:10.1111/j.1600-0854.2010.01032.x. PMID:20059748

[18] Walkley SU, Baker HJ. Sphingomyelin lipidosis in a cat: Golgi studies. Acta Neuropathol. 1984;65:138-144. doi:10.1007/BF00690467. PMID:6441439

[19] Baker HJ, Wood PA, Wenger DA, Walkley SU, Inui K, Kudoh T, Rattazzi MC, Riddle BL. Sphingomyelin lipidosis in a cat. Vet Pathol. 1987;24:386-391. doi:10.1177/030098588702400504. PMID:3672804

[20] Higashi Y, Murayama S, Pentchev PG, Suzuki K. Cerebellar degeneration in the Niemann-Pick type C mouse. Acta Neuropathol. 1993;85:175-184. doi:10.1007/BF00227765. PMID:8382896

[21] Zaaraoui W, Crespy L, Rico A, Faivre A, Soulier E, Confort-Gouny S, Cozzone PJ, Pelletier J, Ranjeva JP, Kaphan E, et al. In vivo quantification of brain injury in adult Niemann-Pick Disease Type C. Mol Genet Metab. 2011;103:138-141. doi:10.1016/j.ymgme.2011.02.013. PMID:21397539